Pan and Xu
Journal of Analytical Science and Technology (2024) 15:2
https://doi.org/10.1186/s40543-024-00415-7

Journal of Analytical Science and Technology

RESEARCH ARTICLE Open Access

A simple and label-free proximity-catalytic hairpin reaction-based method for sensitive and miRNA analysis

Yanyan Pan[1] and Yehong Xu[2*]

Abstract

Aberrant expression of microRNAs (miRNAs) has been shown to be linked to several crucial biological processes, including as carcinogenesis, metastasis, and progression. The advancement of innovative miRNA detection technologies can enhance the early detection of malignancies by merging with conventional diagnostic methods, such as ultrasound technology. Herein, we reported a simple, sensitive, and label-free miRNA detection method by integrating the proximity-catalytic hairpin assembly (proximity-CHA) and DNAzyme-assisted signal amplification. Compared with traditional CHA, in which the signal amplification efficiency is greatly limited by the concentration of hairpin probes, the proposed method possesses a greatly improved signal amplification efficiency. The target facilitated the non-enzymatic CHA-driven sequential formation of DNAzyme nanostructures, resulting in the effective DNAzyme-facilitated cleavage of a substrate modified with a fluorophore and quencher, leading to the production of an intensified fluorescence signal. The proximity-CHA-DNAzyme system possesses appealing analytical characteristics, making it highly promising for the analysis of many analytes in clinical research domains.

Keywords Proximity-catalytic hairpin assembly (proximity-CHA), miRNA, Label-free, Ultrasound technology

Introduction

MicroRNAs (miRNAs) are short RNA molecules that naturally occur in cells and consist of approximately 19–22 nucleotides. They play a role in regulating cell proliferation, differentiation, and death (Ferragut Cardoso et al. 2021; Ho et al. 2022; Saliminejad et al. 2019). The advancement of molecular biology and other technologies has proven the correlation between abnormal miRNA expression and the onset and progression of several diseases (Osaki et al. 2015; Tutar 2014). One important group of miRNAs is miRNA-21, which has alterations in its expression levels that significantly contribute to the development of tumors (Zhou et al. 2018; Shah et al. 2016). These mutations can either promote or suppress the growth of cancer cells. Uterine fibroids (UFs) are non-cancerous growths that occur most frequently in the female reproductive system (Ciebiera et al. 2020). Although ultrasonography is commonly used as the initial imaging method, the development of new biomarkers is crucial for assessing the malignancy of tumors (Cruz and Buchanan 2017). Hence, it is imperative to devise simple, rapid, economical, and highly responsive techniques for miRNA detection.

However, miRNAs are often at low levels in cells, particularly in early-stage cancer cells, making it difficult for classic non-amplified sensing systems to detect. Various signal amplification systems utilizing enzymes, such as polymerase chain reaction (PCR) (Takei et al. 2020; Hu et al. 2021; Zhao et al. 2015) and rolling circle amplification (RCA) (Tian et al. 2019; Wang et al. 2020;

*Correspondence:
Yehong Xu
Yehong_Xu@yeah.net
[1] Medical Ultrasound Center, Northwest Women's and Children's Hospital, Xi'an 710061, Shaanxi, China
[2] Department of Obstetrics, Northwest Women's and Children's Hospital, No. 1616 Yanxiang Road, Qujiang New District, Xi'an 710061, Shaanxi, China

Zhang et al. 2020; Zhang et al. 2018), have been developed. Nevertheless, the traditional PCR method necessitates temperature cycling, which poses difficulties for doing examination within living cells. The isothermal RCA approach requires enzymes that may be vulnerable to the intricate cellular milieu in their vicinity (Zhang et al. 2018; Qiu et al. 2017). Hence, additional endeavors are required to advance the development of novel isothermal signal amplification techniques that do not rely on enzymes, such as hybridization chain reactions (HCR) (Long et al. 2024; Wang et al. 2022), catalytic hairpin assembly (CHA) (Ma et al. 2021; Wu et al. 2021), and DNAzyme catalytic reactions (Yang et al. 2022). Many of the existing methods necessitate the isolation of miRNA from cells before analysis, which prevents real-time monitoring of intracellular miRNA. These enzyme-free methodologies offer potential methods for bioanalysis applications because to their advantages in simplicity, robustness, and thermal stability. Of all the enzyme-free amplification methods, CHA stands out as a unique isothermal reaction driven by free energy. In this reaction, an initiator facilitates the cross-opening of two DNA hairpins, resulting in the production of multiple double-stranded DNA (dsDNA) molecules. The notable characteristics of CHA, such as its uncomplicated design and minimal interference, allow for its wide-ranging use in the amplified detection of diverse nucleic acids (e.g., DNA and RNA), tiny molecules (e.g., adenosine), and proteins (e.g., thrombin). However, traditional CHA-based biomarker detection techniques lack sufficient detection efficiency. There are two alternative strategies that can improve CHA-based amplifying methods, including (i) the proximity of the hairpin probe can significantly improve the chain replacement efficiency in CHA process; (ii) integrate with other signal amplification strategies to improve detection sensitivity.

Catalytic DNA molecules, such as DNAzymes, are gaining increasing attention as amplifying labels for biosensing events (Zeng et al. 2022; Gong et al. 2022). The ability to include functional and structural information into DNA sequences, combined with the reduced tendency of nucleic acids to bind non-specifically, makes them highly versatile for a broad range of applications in domains such as bioanalysis and biomedicine (Nie et al. 2022; Hosseinzadeh et al. 2020). Compared to protein enzymes, DNAzymes possess inherent advantages in terms of their design flexibility and cost-effectiveness. DNAzymes have been successfully utilized in the development of several label-free techniques (Zhang et al. 2017; Zhou et al. 2016).

Herein, an enzyme-free isothermal proximity-CHA-DNAzyme system was developed for nucleic acid analysis by coupling the CHA circuit with a DNAzyme-mediated amplifier as well as transducer. In the present strategy, two hairpins were linked by a single-stranded DNA (ssDNA) sequences to induce the proximity CHA. The proximity of the two hairpin probes endows a high chain replacement efficiency. The target mediates the proximity-CHA-catalyzed hybridization of these functional hairpins to generate plenty of DNAzyme biocatalysts, resulting in an amplified readout signal. As a simple sensing strategy, the proximity-CHA-activated DNAzyme system enabled the sensitive miRNA-21 assay with a low detection limit.

Experimental section

Reagents and apparatus

DNA oligonucleotides were synthesized and HPLC purified by Sangon Biotechnology Co., Ltd. (Shanghai, China); miRNA-21 was obtained from Takara (Dalian, China), and its sequences are listed in Additional file 1: Table S1, DNA and RNA sequences used in this work. All oligonucleotides were dissolved in TE buffer (pH 8.0, 10 mM Tris–HCl, 1 mM EDTA) and stored at − 20 °C, which were diluted in hybridization buffer (20 mM Tris–HCl contains 100 mM NaCl, pH 7.5) prior to use. Fluorescence measurements were performed through the Hitachi fluoro-spectrophotometer F-7000 (Tokyo, Japan).

Fluorescence assay to verify the assembly of hairpin probes

Each functional hairpin (10 μM in 10 mM hybridization buffer, pH 7.5) was heated to 95 °C for 5 min and then allowed to cool to room temperature (25 °C) for 2 h. The successive fluorescence changes were monitored at a fixed emission wavelength of 520 nm upon a fixed excitation of 490 nm (FAM analysis).

Analytical performance of the approach

All samples were prepared in 20 mM TE buffer. The as-prepared hairpins DH probe (100 nM), H3 (20 nM), and H4 (20 nM), and "Reporter" probes (20 nM) were incubated with miRNA-21 for 30 min. The successive fluorescence changes were monitored at a fixed emission wavelength of 520 nm upon a fixed excitation of 490 nm (FAM analysis).

Results and discussion

Principle of isothermal integrated proximity-CHA-DNAzyme system

Here, we report on an isothermal proximity-enzyme-free nucleic acid signal amplified detection based on CHA-mediated DNAzyme assembly. As illustrated in Fig. 1, the present sensing system is based on the design of dual hairpin probe (DH probe). The DH probe is constructed by the assembly of two hairpin probes to a ssDNA

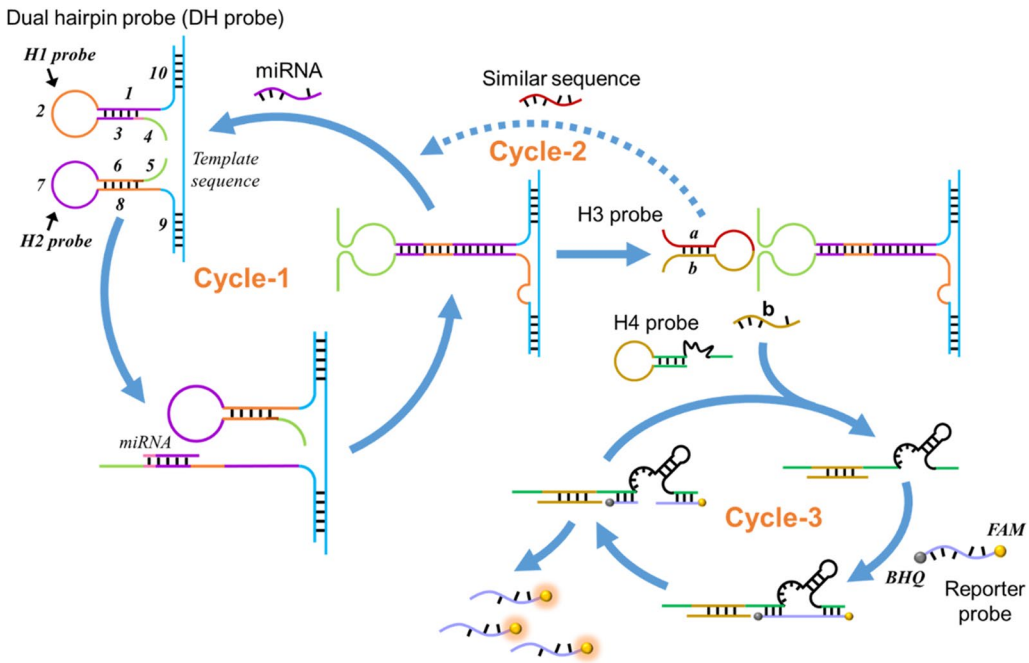

Fig. 1 Principle of isothermal integrated proximity-CHA-DNAzyme system

template sequences through the "9" and "10" fragment. The system consists a ribonucleobase (rA)-containing DNAzyme substrate (H3 probe). The H3 probe contains two functional fragments, including the "**a**" fragment that is similar to the target miRNA and the "b" fragment that initiates subsequent signal amplification.

Each of the two hairpins in DH probe includes a domain that correspond to the complement subunits of the Mg^{2+}-dependent RNA-cleaving DNAzyme. The partial participation of the DNAzyme subunits into the stems of hairpins H1 and H2 blocks the assembly of a catalytically active DNAzyme structure. The target miRNA opens hairpin H1 via a toehold-mediated strand displacement, leading to the formation of miRNA-H1 hybrid. The newly exposed sticky sequence "2" of H1 docks to the "6" fragment of H2 and then opens H2 via branch-migration, leading to the assembly of H1-H2 duplex DNA (dsDNA) and the regeneration of analyte miRNA-21 for CHA reaction. The resulting H1-H2 hybrid includes catalytically active DNAzyme units at the end of the duplex DNA. Thus, target miRNA stimulates the efficient CHA reaction, leading to the successive hybridizations between hairpins H1 and H2, and continuously generating H1-H2 product. The Mg^{2+} binds to the enzyme active site of DNase and activates its substrate cutting properties. In the presence of Mg^{2+} ions, the DNAzyme recognizes and cleaves its H3 probe. The "**a**" fragment in H3 probe is similar to the target miRNA, which is released to initiate a next signal cycle after DNAzyme-based cleavage. The "**b**" fragment unfolds the H4 probe which possesses a DNAzyme toehold. "Reporter probe" is the substrate strand of 8–17 DNAzyme, which labels FAM (6-carboxyfluorescein) and BHQ-1 (Black Hole Quencher) at both ends, respectively. The active DNAzyme can bind and autonomously cleave the substrate strand "Reporter probe" with the help of Mg^{2+}. As a result, FAM is separated from BHQ-1 and generates an enhanced fluorescence signal.

Feasibility of the proximity-CHA and DNAzyme-assisted signal amplification

H1 and H2 probes are assembled into hairpin structures and play an important role in the CHA process. In addition, H1 and H2 probes are fixed to the template chain by "9" and "10" and assembled into DH probes. In order to study the assembly of H1 and H2 probes, fluorescence experiments were performed. In detail, the two terminus of the H1 probe are labeled with FAM and BHQ, and the two terminus of the H2 probe are labeled with Cy5 and BHQ. The two probes (H1 and H2 probes) were heated to 90 °C for 5 min and then slowly cooled to room temperature. Fluorescence signals before and after post-assembly were detected and compared. As shown in Fig. 2A, the fluorescence intensity at wavelength 520 nm (FAM) and 625 nm (Cy5) was significantly reduced when H1 and H2 were assembled, suggesting that H1 and H2 probes were assembled into hairpin structures. To test the assembly of the DH

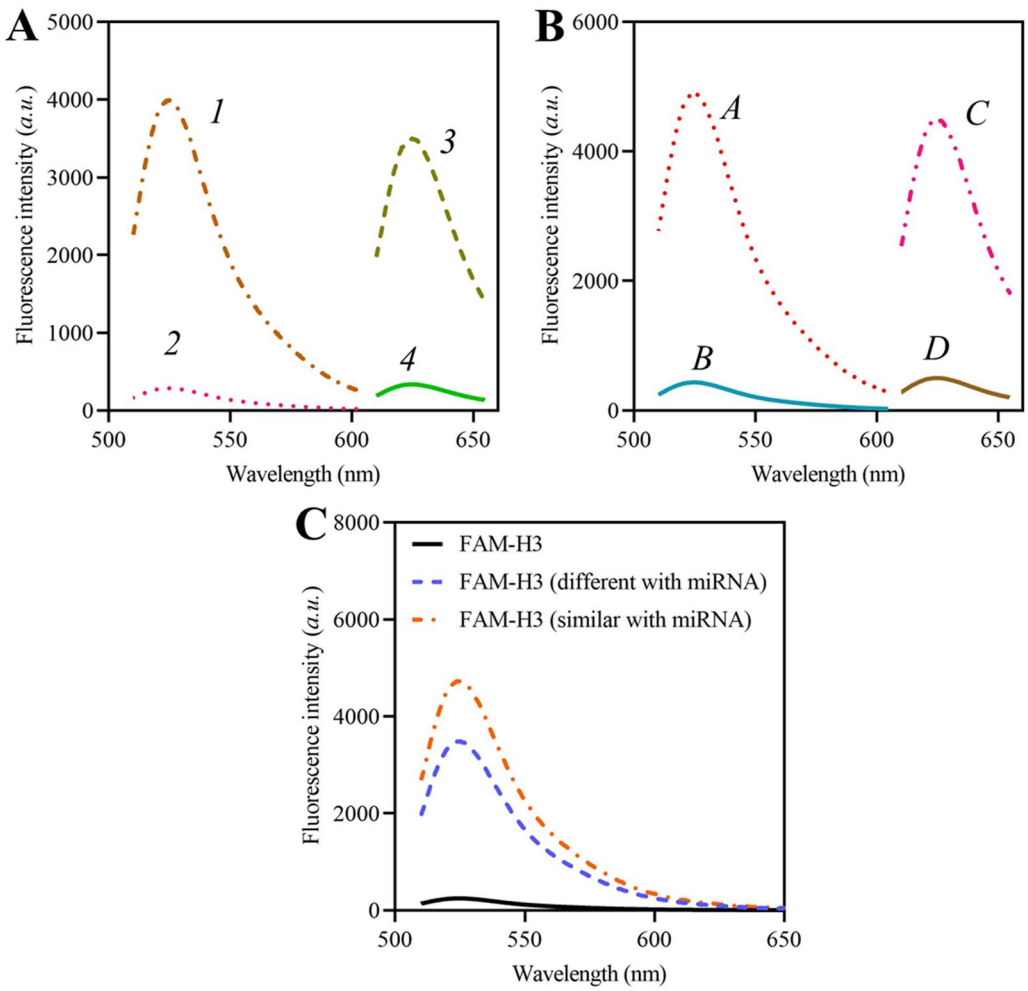

Fig. 2 Feasibility of the proximity-CHA and DNAzyme-assisted signal amplification. **A** Fluorescent spectrum of the FAM labeled H1 probe and Cy5 labeled H2 probe before and after assembly. *1*: H1 probe (linear), *2*: H1 probe (hairpin), *3*: H2 probe (linear), *4*: H2 probe (hairpin). **B** Fluorescent spectrum of the FAM labeled H1 probe and Cy5 labeled H2 probe before and after assembly. *A*: FAM-H1, *B*: FAM-H1 + template sequence, *C*: Cy5-H2, *D*: Cy5-H2 + template sequence. **C** Fluorescent spectrum of the FAM labeled H3 probe with the "a" fragment similar or different with the target miRNA

probe, BHQ is labeled at 3′ terminus of the H1 probe, FAM is labeled at 5′ terminus of the H2 probe, and BHQ and Cy5 are labeled at 3′ end and 5′ end of the template chain, respectively. As shown in Fig. 2B, the signals of FAM and Cy3 decreased significantly when H1 and H2 probes were fixed on the template chain, indicating that H1 probes were fixed on the 5′ end of the template chain and H2 probes were fixed on the 3′ end of the template chain. Fluorescence experiments were used to verify the target catalytic assembly of H1 and H2 probes. In detail, both ends of the H2 probe are labeled with fluorophores and quenched groups, respectively. When the H2 probe is hairpin structure, the fluorescence signal is kept at a low level. When H2 probe is mixed with the H1 probe, no significant enhancement of fluorescence signal was observed. Significant fluorescence signal enhancement is found only when the target miRNA is present, suggesting that the H2 probe is unfolded and the catalytic hairpin assembly is performed (Additional file 1: Fig. S1, Fluorescence intensity of the H2 probe during the catalytic hairpin assembly between H1 probe and H2 probe). Both ends of the H3 probe label FAM and BHQ respectively to validate DNAzyme-based substrate cuts. When the H3 probe was assembled into a hairpin structure, the FAM signal was quenched by BHQ. When the target is present, the tail ends of H1 and H2 are assembled into a complete DNAzyme-cut H3 probe. As a result, the FAM labeled "a" segment was released and the FAM signal reappeared (Fig. 2C). To verify the value

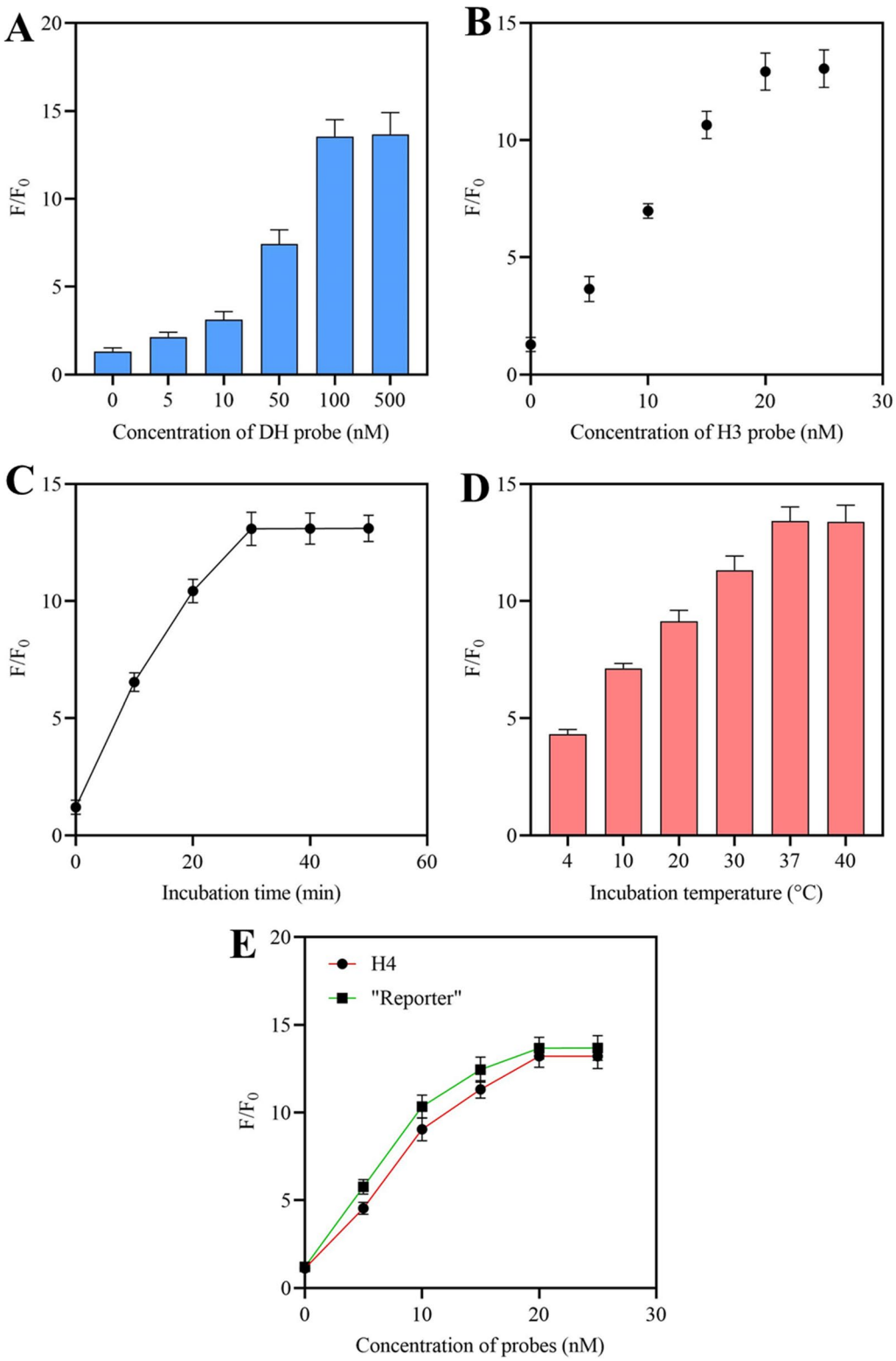

Fig. 3 Optimization of experimental parameters. Fluorescence ratio (F/F_0) of the approach when detecting miRNA with different DH concentrations (**A**), H3 probe concentrations (**B**), incubation time (**C**), temperature (**D**), H4 probe concentration, and "Reporter" probe concentrations (**E**)

of designing the "a" fragment to be similar to miRNA in improving signal amplification, we compared the results when the "a" fragment was similar to or not similar to miRNA. Figure 3 shows that when the "a" fragment is similar to miRNA, the recorded signal is improved by about 35%.

Optimization of experimental parameters

Numerous parameters were optimized in order to achieve the highest level of sensing performance for the proximity-CHA-DNAzyme-based biosensor designed to detect miRNA-21. The developed biosensor's performance was evaluated using the signal-to-noise ratio (F/F_0). The concentration of the DH probe may significantly impact the cascade CHA process. Consequently, we initially optimized the concentration of DH probes. The signal-to-noise ratio exhibited enhancement as the concentration of DH probes escalated from 0 to 100 nM, subsequently attaining a state of equilibrium (Fig. 3A). The concentration of the H3 probe may also have a significant impact on facilitating the subsequent signal amplification. The ideal concentration of the H3 probe was determined to be 20 nM, as it yielded the maximum signal-to-noise ratio (Fig. 3B). Next, the impact of the incubation time of CHA is examined in Fig. 3C. The signal-to-noise ratio peaked at 30 min, therefore making it the optimal incubation duration. Furthermore, the temperature ranges of 4 °C to 47 °C were investigated (Fig. 3D), and the optimal signal-to-noise ratio was attained at 37 °C. Therefore, it was concluded that the ideal incubation temperature for the subsequent experiments is 37 °C. Furthermore, as the signal output was affected by both the H4 probe and the "Reporter" probe, we also examined concentrations of these two probes. The result in Fig. 3E demonstrated the optimal concentrations of the H4 probe and the "Reporter" probe of 20 nM each. The concentration of Mg^{2+} can affect the efficiency of DNAzyme in cutting substrates, thereby affecting experimental results. Therefore, the concentration of Mg^{2+} was optimized and determined 2 μM (Additional file 1: Fig. S2, Fluorescence ratio (F/F0) of the approach when detecting miRNA with different Mg2+ concentrations).

Dynamic range, sensitivity, and selectivity for miRNA detection

The dynamic range and sensitivity of the proposed sensor were verified under the ideal experimental conditions. Figure 4A demonstrates a positive correlation between the concentration of target miRNA and the fluorescence signals, indicating that higher concentrations of the miRNA result in stronger fluorescence signals. The calibration plots exhibited a strong linear correlation between the peak fluorescence intensities and the logarithm of target miRNA concentrations within the range of 10 fM to 1 nM (Fig. 4B). The linear regression equation, F (a.u.) = 708.9*lgC-131.2, had a correlation coefficient of 0.9945. The low detection limit was determined to be 3.2 fM, which was calculated as three times the standard deviation of the blank sample detection. These findings indicate that the equation is adequate for analyzing miRNA actual samples. The results demonstrate that our technique exhibits enhanced sensitivity in comparison with conventional CHA. The enhanced signal amplification effectiveness of proximity-CHA and DNAzyme-assisted signal amplification is primarily responsible for the achieved excellent detection limit and sensitivity.

In order to evaluate the selectivity of the devised approach, the approach was applied for the detection of sequence that possesses a single-base mismatch (SM) with the target miRNA target, interfering miRNAs, and target miRNA (all at a concentration of 50 pM). Figure 4C demonstrates that the presence of the target miRNA led to a considerably stronger signal response compared to the single-base mismatched target (SM), with a computed fluorescence intensity of 148.2 a.u., demonstrating that the biosensor exhibited exceptional selectivity in detecting the specific miRNA of interest. Detecting the low concentrations of miRNA target from interfering miRNAs with significantly higher concentrations continues to be an immense problem, to assess the assay's capability to detect the seldom miRNA target. Specifically, we studied a combination containing 50 pM of a miRNA target, along with interference miRNAs that have similar sequences with a 20-fold higher concentration (1 nM). Figure 4D demonstrates that the 50 pM pure miRNA target exhibited a significant fluorescence reaction, whereas the spurious miRNA target had a response identical to the blank. The aforementioned findings illustrate that our suggested biosensor exhibits the capacity to identify infrequent miRNA with a rarity of 5%.

Real sample analysis

The RNA lysate solutions obtained from the MCF-7 and HeLa human cancer cell lines were used to assess the ability of the developed bio-sensing technology to detect miRNA-21 in actual biological samples. Figure 5A shows that the signal response rose as the number of cells grew, demonstrating a clear expression level of miRNA-21 in MCF-7. However, no significant responses were found in blank samples and HeLa cells, indicating a lower expression level compared to MCF-7. The aforementioned findings were in line with prior studies, providing further evidence that the measurement of miRNA-21 in cancer cells has significant promise for the clinical detection of malignancies. The accuracy of the method was validated

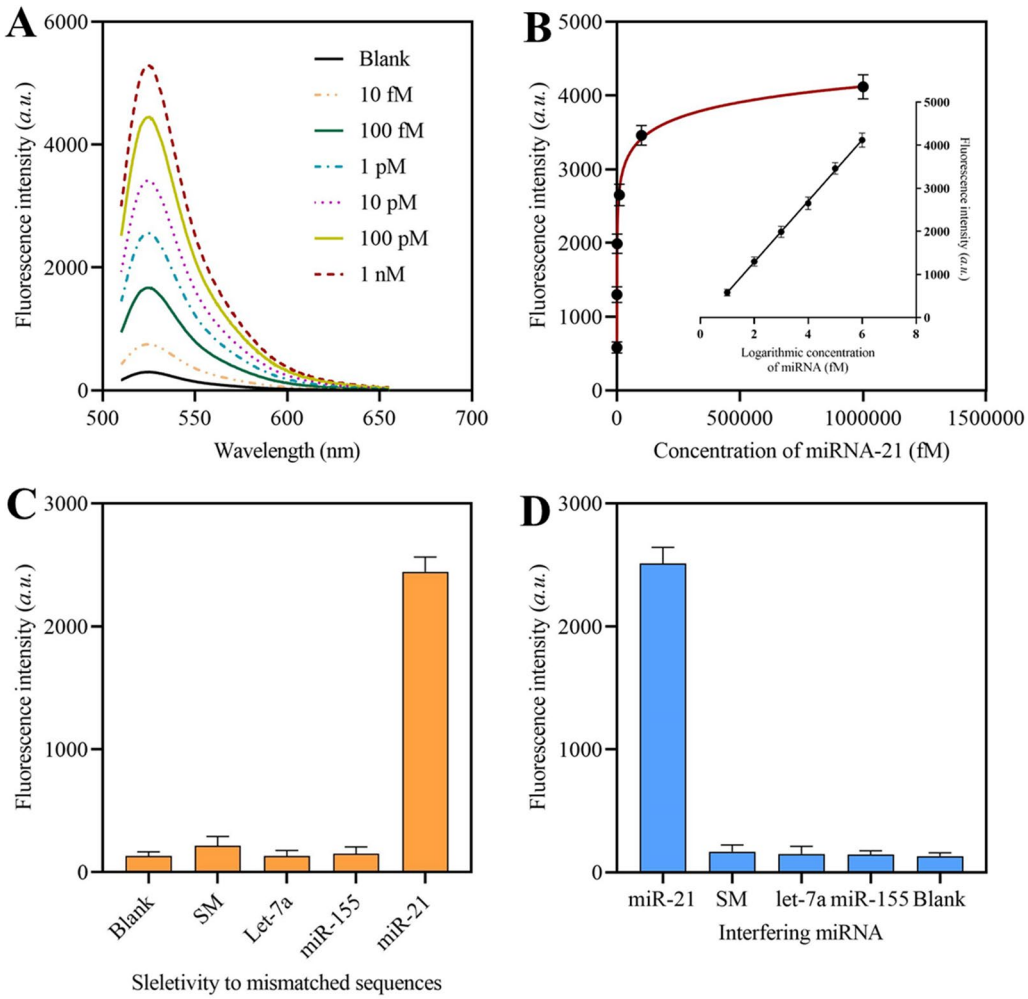

Fig. 4 Analytical performance of the approach for miRNA analysis. **A** Fluorescent spectrum of the approach when detecting different concentrations of miRNA. **B** Correlation between the recorded fluorescence intensity and the concentration of miRNA. **C** Fluorescence intensities of the approach when detecting different miRNA. **D** Fluorescence intensities of the approach when detecting interfering miRNA with 20-fold higher concentrations

by detecting miRNAs in artificial blood samples. For the construction of artificial blood samples, different concentrations of miRNA were diluted in commercial serum samples. As shown in Fig. 5B, this method only showed a very high signal response to the target miRNA, indicating high selectivity in clinical samples.

Conclusion

Our proposed strategy of integrating proximity-CHA with DNAzyme-assisted signal amplification offers improved signal amplification efficiency compared to traditional nucleic acid signal amplification methods. This leads to faster reaction speed and higher detection sensitivity in the hybridization reaction, surpassing those of traditional CHA-based methods. Utilizing these benefits, the biosensor is effectively utilized as a highly efficient DNA signal amplifier to create an immobilization-free biosensor for the rapid and extremely sensitive detection of miRNA-21. The low detection limit was determined to be 3.2 fM, which is superior or comparable to former miRNA detection methods (Additional file 1: Table S2, Comparison of the approach with former methods). This paves the way for a novel approach in designing a potential strategy for bio-sensing assays and clinical diagnosis. In addition, the biosensor offers a novel perspective on harnessing the intrinsic capability of nucleic acid amplification to enhance its superiority and usefulness in diagnostic applications, biological research, and other related fields. The use of ultrasonic diagnosis is prevalent in tumor screening due to its minimal impact on the human body and

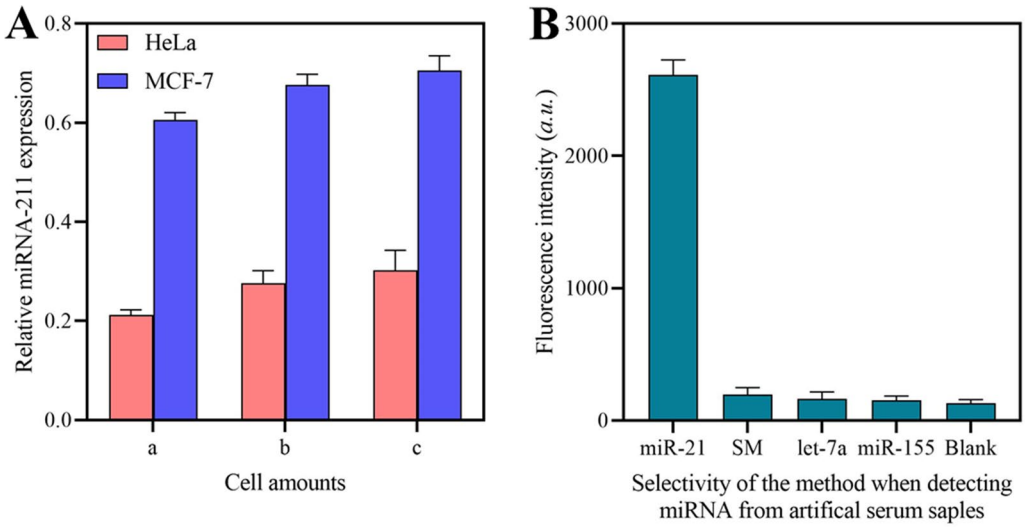

Fig. 5 Clinical application potential of the approach. **A** Relative miRNA-21 expression calculated by the approach from different amounts of HeLa and MCF-7 cells. a, HeLa (100 cells) and MCF-7 (100 cells); b, HeLa (1000 cells) and MCF-7 (1000 cells); c, HeLa (10 000 cells) and MCF-7 (10 000 cells). **B** Fluorescence intensities of the approach when detecting miRNA from artificial serum samples

straightforward procedure. However, ultrasonography technology lacks the ability to differentiate between benign and malignant tumors. Alternatively, the developed miRNA detection method can enhance the utilization of ultrasound technology in tumor diagnostics.

Supplementary Information

The online version contains supplementary material available at https://doi.org/10.1186/s40543-024-00415-7.

Additional file 1. Supplementary material, tables and figures.

Author contributions

YX is the supervisor of the team in all research steps including designing, data analysis, and manuscript writing. YP, as the first author, has the main role for experimental data collection, data gathering, preparation of results, and data analysis.

Funding

No fund available.

Availability of data and materials

Almost all details of experimental data are presented in the article or additional file.

Declarations

Ethics approval and consent to participate

The manuscript does not contain clinical or trial studies on patients, humans, or animals.

Competing interests

The authors declare that they have no competing interests.

Received: 13 December 2023 Accepted: 3 January 2024
Published online: 12 January 2024

References

Ciebiera M, Wlodarczyk M, Zgliczynski S, Lozinski T, Walczak K, Czekierdowski A. The role of miRNA and related pathways in pathophysiology of uterine fibroids-from bench to bedside. Int J Mol Sci. 2020; 21(8)

De La Cruz MS, Buchanan EM. Uterine fibroids: diagnosis and treatment. Am Fam Physician. 2017;95(2):100–7.

Ferragut Cardoso AP, Banerjee M, Nail AN, Lykoudi A, States JC. miRNA dysregulation is an emerging modulator of genomic instability. Semin Cancer Biol. 2021;76:120–31.

Gong H, Hu X, Zeng R, Li Y, Xu J, Li M, Tang D. CRISPR/Cas12a-based photoelectrochemical sensing of microRNA on reduced graphene oxide-anchored Bi2WO6 coupling with catalytic hairpin assembly. Sens Actuators B Chem 2022; 369.

Ho PTB, Clark IM, Le LTT. MicroRNA-based diagnosis and therapy. Int J Mol Sci 2022**,** 23 (13).

Hosseinzadeh E, Ravan H, Mohammadi A, Pourghadamyari H. Colorimetric detection of miRNA-21 by DNAzyme-coupled branched DNA constructs. Talanta. 2020;216: 120913.

Hu C, Zhang L, Yang Z, Song Z, Zhang Q, He Y. Graphene oxide-based qRT-PCR assay enables the sensitive and specific detection of miRNAs for the screening of ovarian cancer. Anal Chim Acta. 2021;1174: 338715.

Long K, Cao G, Qiu Y, Yang N, Chen J, Yang M, Hou C, Huo D. Hybridization chain reaction circuit controller: CRISPR/Cas12a conversion amplifier for miRNA-21 sensitive detection. Talanta. 2024;266(Pt 2): 125130.

Ma GM, Huo LW, Tong YX, Wang YC, Li CP, Jia HX. Label-free and sensitive MiRNA detection based on turn-on fluorescence of DNA-templated silver nanoclusters coupled with duplex-specific nuclease-assisted signal amplification. Mikrochim Acta. 2021;188(10):355.

Nie N, Tang W, Ding X, Guo X, Chen Y. DNAzyme based dual signal amplification strategy for ultrasensitive myocardial ischemia related MiRNA detection. Anal Biochem. 2022;640: 114543.

Osaki M, Okada F, Ochiya T. miRNA therapy targeting cancer stem cells: a new paradigm for cancer treatment and prevention of tumor recurrence. Ther Deliv. 2015;6(3):323–37.

Qiu Z, Shu J, He Y, Lin Z, Zhang K, Lv S, Tang D. CdTe/CdSe quantum dot-based fluorescent aptasensor with hemin/G-quadruplex DNzyme for sensitive detection of lysozyme using rolling circle amplification and strand hybridization. Biosens Bioelectron. 2017;87:18–24.

Saliminejad K, Khorram Khorshid HR, Soleymani Fard S, Ghaffari SH. An overview of microRNAs: Biology, functions, therapeutics, and analysis methods. J Cell Physiol. 2019;234(5):5451–65.

Shah S, Jadhav K, Shah V, Gupta N, Dagrus K. miRNA 21: diagnostic prognostic and therapeutic marker for oral cancer. Microrna. 2016;5(3):175–9.
Takei F, Akiyama M, Murata A, Sugai A, Nakatani K, Yamashita I. RT-Hpro-PCR: a MicroRNA detection system using a primer with a DNA tag. ChemBioChem. 2020;21(4):477–80.
Tian W, Li P, He W, Liu C, Li Z. Rolling circle extension-actuated loop-mediated isothermal amplification (RCA-LAMP) for ultrasensitive detection of microRNAs. Biosens Bioelectron. 2019;128:17–22.
Tutar Y. miRNA and cancer; computational and experimental approaches. Curr Pharm Biotechnol. 2014;15(5):429.
Wang R, Zhao X, Chen X, Qiu X, Qing G, Zhang H, Zhang L, Hu X, He Z, Zhong D, Wang Y, Luo Y. Rolling circular amplification (RCA)-assisted CRISPR/Cas9 cleavage (RACE) for highly specific detection of multiple extracellular vesicle MicroRNAs. Anal Chem. 2020;92(2):2176–85.
Wang Y, Feng H, Huang K, Quan J, Yu F, Liu X, Jiang H, Wang X. Target-triggered hybridization chain reaction for ultrasensitive dual-signal miRNA detection. Biosens Bioelectron. 2022;215: 114572.
Wu Y, Fu C, Shi W, Chen J. Recent advances in catalytic hairpin assembly signal amplification-based sensing strategies for microRNA detection. Talanta. 2021;235: 122735.
Yang H, Weng B, Liu S, Kang N, Ran J, Deng Z, Wang H, Yang C, Wang F. Acid-improved DNAzyme-based chemiluminescence miRNA assay coupled with enzyme-free concatenated DNA circuit. Biosens Bioelectron. 2022;204: 114060.
Zeng R, Xu J, Lu L, Lin Q, Huang X, Huang L, Li M, Tang D. Photoelectrochemical bioanalysis of microRNA on yolk-in-shell Au@CdS based on the catalytic hairpin assembly-mediated CRISPR-Cas12a system. Chem Commun. 2022;58(54):7562–5.
Zhang K, Lv S, Lin Z, Tang D. CdS: Mn quantum dot-functionalized g-C(3) N(4) nanohybrids as signal-generation tags for photoelectrochemical immunoassay of prostate specific antigen coupling DNAzyme concatamer with enzymatic biocatalytic precipitation. Biosens Bioelectron. 2017;95:34–40.
Zhang K, Lv S, Lin Z, Li M, Tang D. Bio-bar-code-based photoelectrochemical immunoassay for sensitive detection of prostate-specific antigen using rolling circle amplification and enzymatic biocatalytic precipitation. Biosens Bioelectron. 2018;101:159–66.
Zhang GZL, Tong J, Zhao X. Ren J (2020) CRISPR-Cas12a enhanced rolling circle amplification method for ultrasensitive miRNA detection. Microchem J. 2020;158:105239.
Zhao Y, Chen F, Li Q, Wang L, Fan C. Isothermal amplification of nucleic acids. Chem Rev. 2015;115(22):12491–545.
Zhou Q, Lin Y, Lin Y, Wei Q, Chen G, Tang D. Highly sensitive electrochemical sensing platform for lead ion based on synergetic catalysis of DNAzyme and Au–Pd porous bimetallic nanostructures. Biosens Bioelectron. 2016;78:236–43.
Zhou Y, Ren H, Dai B, Li J, Shang L, Huang J, Shi X. Hepatocellular carcinoma-derived exosomal miRNA-21 contributes to tumor progression by converting hepatocyte stellate cells to cancer-associated fibroblasts. J Exp Clin Cancer Res. 2018;37(1):324.

Publisher's Note